Journal of Porphyrins and Phthalocyanines

Article Title: **Zinc Porphyrins-Anthraquinonylimidazoles supramolecular dyads**

Author(s): **Federica Sabuzi, Alessia Coletti, Valeria Conte, Barbara Floris, Pierluca Galloni**

DOI: **10.1142/S1088424619501943**

To be cited as:

Federica Sabuzi, Alessia Coletti, Valeria Conte, Barbara Floris, Pierluca Galloni, Zinc Porphyrins-Anthraquinonylimidazoles supramolecular dyads, *Journal of Porphyrins and Phthalocyanines*, doi: 10.1142/S1088424619501943

Received: **6 November, 2019**
Accepted: **5 December, 2019**

Zinc Porphyrins-Anthraquinonylimidazoles supramolecular dyads

Federica Sabuzi[#], Alessia Coletti[#], Valeria Conte, Barbara Floris and Pierluca Galloni*

Department of Chemical Sciences and Technologies, University of Rome Tor Vergata, Via della Ricerca Scientifica snc, 00133 Rome, Italy

Dedicated to Professor Roberto Paolesse on the occasion of his 60th birthday

Received date (to be automatically inserted after your manuscript is submitted)
Accepted date (to be automatically inserted after your manuscript is accepted)

ABSTRACT: In this work, the synthesis and spectroscopic characterization of new zinc porphyrins – anthraquinones dyads is proposed. In particular, electron donor units based on zinc *meso*-tetraphenylporphyrin (**ZnTPP**) and zinc octaethylporphyrin (**ZnOEP**) have been coupled with differently substituted anthraquinones as acceptors. The quinone moiety was properly functionalized with imidazole, thus ensuring porphyrin complexation through zinc ion coordination. Accordingly, absorption and emission measurements demonstrated that the coordination occurred, and calculated binding constants were in the range $6.6 \cdot 10^3$ - $3.9 \cdot 10^4$ M^{-1}. Transient absorption spectroscopy for **ZnTPP** and **ZnOEP** dyads demonstrated that the electron transfer occurred, with the formation of the corresponding charge separated state, **$ZnTPP^+$-AQ^-**. Moreover, in **ZnOEP** complexes, a strong correlation between the chain length and flexibility with the charge separated state lifetime was observed.

KEYWORDS: zinc tetraphenylporphyrin, zinc octaethylporphyrin, anthraquinones, dyads, electron transfer.

*Correspondence to: Pierluca Galloni, tel +390672594380, fax +390672594328 email galloni@scienze.uniroma2.it
#these two authors contributed equally

INTRODUCTION

To mimic the natural photosynthesis has been a goal pursued by scientists for many years. Nowadays, it is common knowledge that the simplest chemical system has to be formed by at least two moieties, an electron donor and an electron acceptor unity, connected in a variety of ways. A 2019 review discussed more than 150 papers relative to organic electron Donor-Acceptor (D-A) dyads and their features (charge separation and recombination, long-lived charge transfer states, intersystem crossing) [1]. Computational models were developed as a tool for a rational design of covalently linked dyads [2]. However, the way to D-A dyads as efficient as natural systems is still long. Porphyrins and zinc porphyrins have been the donors of choice in most cases, being the molecules closest to the natural system, whereas a wide range of acceptors were investigated. Apart from fullerenes, for which a plethora of papers appeared (to cite only a few in the last three years see [3-11]), a wide range of acceptor structures were investigated, from naphthalenediimide [12, 13] to coumarin [14] and carbazole [15-17] or corrole [18]. Moreover, a number of papers appeared dealing with porphyrin-quinone D-A dyads. As an example, a free base tetra-*meso*-substituted porphyrin was coupled to anthraquinone via azo functionality [19]. Later, 1,4-benzoquinone was directly linked at the meso position of tri-*meso*-substituted zinc porphyrins [20] or to a cyclohexane ring as a spacer [21]. More complex were the triads published in 2014, with zinc 1,10-diaryl-porphyrins, bearing a *N*-ferrocenyl-4-benzenamide at position 5 and a 4-(2-anthraquinonecarboxylic anilide) at position 15 [22]. Finally, zinc porphyrin-anthraquinone dyads were prepared with donor and acceptor covalently linked through different spacers [23].

All these systems suffer of the problem of low yields and difficult preparation methodologies. Therefore, considering our experience in quinoidal systems [24-28] and taking advantage of the coordinating ability of imidazole for the metal of Zn-porphyrins [29,30], we prepared a series of anthraquinone functionalized with different spacers bearing imidazole, in order to obtain porphyrin anthraquinone dyads (**P-AQ**). The donor and acceptor moieties prepared are summarized in Chart 1. In particular, anthraquinone, which is one the most common quinonic systems, has been chosen as the acceptor, whereas zinc *meso*-tetraphenylporphyrin (**ZnTPP**) and zinc octaethylporphyrin (**ZnOEP**) were chosen as the donors, so that electronic and steric effect of substituents could be appreciated. The interaction between the porphyrin and the quinone has been ensured functionalizing the quinone with imidazole, thus allowing the formation of a metal-ligand coordination bond. Three different spacers were used to link the imidazole and the anthraquinone scaffold, in order to change the distance between the donor and the acceptor moieties and the flexibility of the chain. Herein, the study of the photoinduced electron transfer in such new P-AQ dyads is presented.

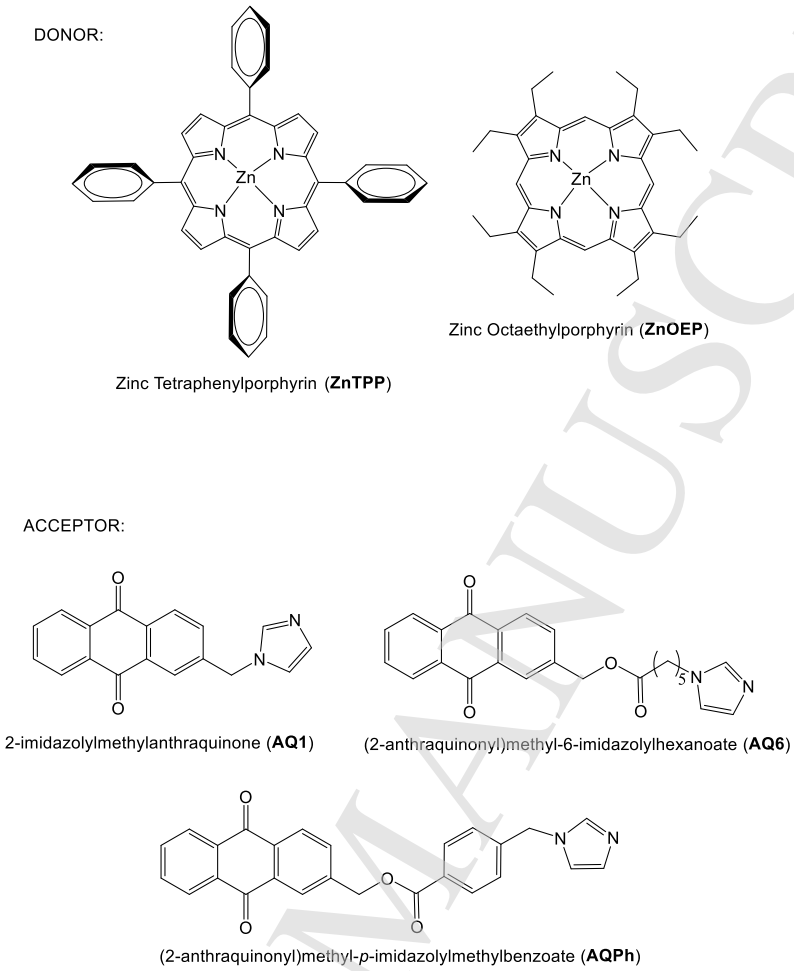

Chart 1. Formulae of porphyrins (donors) and imidazolyl substituted anthraquinones (acceptors) used in **P-AQ** dyads.

EXPERIMENTAL

General

^{1}H-NMR spectra were recorded on a Bruker Avance 300 MHz spectrometer. ^{13}C-NMR spectra were recorded on Bruker 400 MHz spectrometer. LC-MS analysis have been performed with Shimadzu LCMS-2010 EV. UV-visible spectra were recorded on a SHIMADZU 2450 spectrometer equipped with the UV Probe 2.34 program. Fluorescence spectra were recorded on a spectrofluorimeter SPEX 1681 Fluorolog, equipped with two double monochromators (excitation and emission).

Cyclic voltammetries were performed with a Palm Sens instrument using PS Trace software.

Femtosecond pump and probe transient absorption measurements were performed using a Spectra-Physics Hurricane titanium/sapphire regenerative amplified laser system. The full spectrum pumping tunability was based on an optical parametric amplifier (Spectra-Physics OPA 800). A residual fundamental light was used for generation of a white light continuum from a sapphire window (450-1500 nm) as the probe, which was detected with two separated diode array based spectrometers (OceanOptics and Control Development). The laser output (800 nm) was typically 0.8 *i*J pulse-1 (130 fs

fwhm) with a repetition rate of 1 kHz. The OPA was used to generate excitation pulses at different wavelengths (1.5 *i*J pulse-1). To avoid local heating by the laser beam, the sample cuvette (1 mm) was placed on a moving kinematics stage.

Synthesis

Tetraphenylporphyrin and octaethylporphyrin were used as purchased and treated with zinc acetate to form the corresponding zinc complexes, ZnTPP and ZnOEP.

Preparation of zinc-5,10,15,20-meso-Tetraphenylporphyrin (**ZnTPP**). The synthesis of **ZnTPP** was obtained upon complexation of the commercially available free base H_2TPP with $Zn(OAc)_2$ using a slightly modified literature procedure [31]. A solution of 0.6 g (3.3 mmol) of $Zn(OAc)_2$ in 3 mL of MeOH was added to a solution of 204 mg (0.33 mmol) H_2TPP in 10 mL of $CHCl_3$ and the mixture was refluxed under stirring for 3 hours. After disappearance of H_2TPP (TLC analysis), the reaction mixture was washed three times with water, dried with Na_2SO_4 and the solvent was reduced to the minimum volume. After addition of hexane to the concentrated solution, the product crystallized. Yield, 84% (189 mg, 0.28 mmol). ^{1}H-NMR in $CDCl_3$ δ(ppm): 8.96 (s, 8H, pyrrole rings); 8.23 (m, 8H, *orto* positions of the phenyl rings); 7.78 (m, 12H, *para* and *meta* positions of the phenyl rings).

Preparation of zinc-2,3,7,8,12,13,17,18-Octaethylporphyrin (**ZnOEP**). **ZnOEP** was synthesized from 77 mg (0.14 mmol) of the commercially available free base porphyrin H_2OEP and 0.6 mg of $Zn(OAc)_2$ (3.3 mmol) following the procedure described for ZnTPP. To isolate the product, the solvent was evaporated from the reaction mixture and the solid residue was crystallized once from THF-pentane and twice from THF-diethyl ether. Yield, 90% (77 mg, 0.13 mmol). ^{1}H-NMR in $CDCl_3$ δ(ppm): 10.19 (s, 4H, *meso* positions of the porphyrin core); 4.14 (q, 16H, J=7.8Hz, methylene groups); 1.96 (t, 24H, J=7.5Hz, methyl groups).

Preparation of 2-imidazoylmethyl-9,10-anthraquinone (**AQ1**). 300 mg (1 mmol) 2-bromomethyl-9,10-anthraquinone and 137 mg (2 mmol) imidazole were dissolved in 20 mL CH_2Cl_2 previously dried over $CaCl_2$, in anhydrous atmosphere. The solution was kept under stirring overnight and then refluxed for 5 hours. A yellow precipitate was observed that was recovered by filtration, dissolved in $CHCl_3$, and extracted with an aqueous alkaline solution. The organic phase was dried over Na_2SO_4 and filtered and the solvent was distilled under reduced pressure. To purify the product, the solid obtained was dissolved in the minimum amount of $CHCl_3$; after addition of hexane, a precipitate formed that was recovered by filtration and further purified by repeating the same procedure. Yield, 40% (110 mg) ^{1}H-NMR in $CDCl_3$ δ(ppm): 8.34 (m, 3H); 8.17 (d, 1H, J=1.5Hz); 7.84 (m, 2H); 7.64 (s, 1H); 7.53 (dd, 1H, J_1=2Hz, J_2=7Hz); 7.17 (s, 1H); 6.97 (s, 1H); 5.32 (s, 2H). ^{13}C-NMR in CD_3Cl_3 δ(ppm): 182.98 and 182.73 (C=O); 140.35, 136.34, 133.62, 133.46, 132.88, 132.43, 132.13, 130.45, 129.15, 128.85, 126.36, 126.14, 125.86, 123.71 and 119.78 (sp^2 carbons); 53.45 (sp^3 carbon). MS (ESI$^+$ in CH_3CN): 289 ($M+H^+$).

Preparation of (2-anthraquinonyl)methyl 6-bromohexanoate. In a round bottomed flask, kept under nitrogen, 250 mg (1 mmol) 2-hydroxymethyl-9,10-anthraquinone, 100 µL (1.1 mmol) pyridine dried over K_2CO_3 and then 160 µL (1 mmol) 6-bromohexanoyl chloride in 50 mL of CH_2Cl_2 dried over $CaCl_2$ were added. The reaction mixture became completely homogeneous only after the addition of the carbonyl chloride. The solution stirred under anhydrous atmosphere overnight. TLC analysis (SiO_2, CH_2Cl_2 as the eluent) showed uncomplete consumption of the substrate, even after additional 1 hour at

reflux. The reaction mixture was washed four times with water, dried with Na_2SO_4 and the solvent was evaporated. The product was first crystallized with toluene and then purified by column chromatography, using SiO_2 as the stationary phase and CH_2Cl_2 as the eluent. The product obtained was crystallized from dichloromethane-hexane. Yield, 57.7 % (240 mg, 57.7 mmol). ^{1}H-NMR in $CDCl_3$ δ(ppm): 8.35 (m, 3H); 8.30 (d, 1H, *J*=1.5 Hz); 7.84 (m, 2H); 7.78 (dd, 2H, J_1=2.0 Hz, J_2=8.0 Hz); 5.30 (s, 2H); 3.43 (t, 2H, *J*=6.5 Hz); 2.48 (t, 2H, *J*=7.5 Hz); 1.9 (m, 2H); 1.74 (m, 2H); 1.53 (m, 2H).

Preparation of (2-anthraquinonyl)methyl 6-imidazolylhexanoate (**AQ6**). The reaction was carried out in dried glassware and nitrogen atmosphere. 0.5 mmol 2-(6-bromohexanoyloxymethyl)-9,10-anthraquinone were dissolved in 5 mL of anhydrous acetonitrile containing 117 mg (1.1 mmol) of anhydrous Na_2CO_3; 34 mg (0.5 mmol) imidazole was subsequently added. The reaction was refluxed for 24 hours. The formed solid precipitate was recovered by filtration and the solution was distilled and combined with the precipitate. The powder obtained was dissolved in dichloromethane, extracted with water and the organic phase was dried over anhydrous Na_2SO_4 and distilled. The compound was purified by column chromatography, using SiO_2 as the stationary phase and a mixture of 3% v/v CH_3OH in CH_2Cl_2 as the eluent. The first fraction eluted was the compound of interest, that was concentrated and precipited with hexane. Yield, 7.2% (14.5 mg, 0.036 mmol). ^{1}H-NMR in $(CD_3)_2CO$ δ(ppm): 8.29 (m, 4H); 7.95 (m, 3H); 7.56 (s, 1H); 7.1 (s, 1H); 6.9 (s, 1H); 5.36 (s, 2H); 4.06 (t, 2H, *J*=7.2 Hz); 2.49 (t, 2H, *J*=7.2 Hz); 1.84 (m, 2H); 1.72 (m, 2H); 1.38 (m, 2H). ^{13}C-NMR in $(CD_3)_2CO$ δ(ppm): 183.13 and 182.70 (aromatic C=O); 172.80 (aliphatic C=O); 142.76, 135.17, 134.41, 134.35, 133.73, 133.49, 133.43, 133.13, 132.96, 127.85, 127.36, 127.34, 125.76, 120.57 and 120.37 (sp^2 carbons); 65.12, 49.34, 33.67, 30.22, 25.71 and 24.08 (sp^3 carbons). MS (ESI^+ in CH_3CN): 466 ($M+CH_3CN+Na^+$).

Preparation of (2-anthraquinonyl)methyl p-bromomethylbenzoate [32]. 646.2 mg (3 mmol) *p*-bromomethylbenzencarboxylic acid was dissolved in about 5 mL dichloromethane dried over $CaCl_2$ in dried glassware, under gentle stream of nitrogen. 742.8 mg (3.6 mmol) dicyclohexylcarbodiimide (DCC) and 20.3 mg (0.16 mmol) *N*,*N*-dimethylaminopyridine (DMAP) were added with consequent formation of a white precipitate. 715 mg (3 mmol) 2-hydroxymethylanthraquinone was added and the reaction mixture was kept under stirring for 24 hours in anhydrous atmosphere. The reaction mixture was diluted with 100 mL of dichloromethane; the solid dicyclohexylurea formed was removed by filtration and the solvent was distilled. The solid obtained was dissolved with boiling toluene and further filtered, then kept at -18°C overnight. The yellow solid formed was recovered by decantation and further purified by crystallisation with toluene. The compound was pure at TLC analysis (eluent: dichloromethane). Yield, 64% (840 mg, 1.93 mmol). ^{1}H-NMR in $CDCl_3$ δ(ppm): 8.35 (m, 4H); 8.09 (d, 2H, *J*=8.0 Hz); 7.85 (m, 3H); 7.53 (d, 2H, *J*=8.0 Hz); 5.54 (s, 2H); 4.53 (s, 2H).

Preparation of (2-anthraquinonyl)methyl p-imidazolylmethylbenzoate (**AQPh**). 70 mg (1.03 mmol) imidazole was dissolved in 5 mL of CH_2Cl_2 (dried over $CaCl_2$) in dried glassware and, after addition of 235 mg (0.54 mmol) (2-anthraquinonyl)methyl *p*-bromomethylbenzoate, the solution was diluted to 10 mL and kept stirring under anhydrous atmosphere for 3 days. The precipitate and the solution obtained were dissolved in 75 mL of dichloromethane and extracted with NaCl aqueous solution. The organic phase was dried over anhydrous Na_2SO_4, filtered and concentrated until reaching the minimum volume. The compound precipitated upon addition of hexane and recovered by filtration. Yield, 23% (52.1 mg, 0.12 mmol). ^{1}H-NMR in $(CD_3)_2SO$ δ(ppm): 8.35 (m, 4H); 8.09 (d, 2H, *J*=8.0 Hz); 7.85 (m, 3H); 7.78 (s, 1H); 7.53 (d,

2H, *J*=8.0 Hz); 7.21 (s, 1H); 6.93 (s, 1H); 5.54 (s, 2H); 5.43 (s, 2H). ^{13}C-NMR in $CDCl_3$ δ(ppm): 182.53 and 182.10 (aromatic C=O); 169.04 (aliphatic C=O); 145.12, 142.13, 134.98, 134.61, 134.05, 133.65, 133.33, 133.12, 132.83, 132.77, 130.45, 130.12, 129.95, 129,67, 128.34, 127.98, 127.55, 127.11 126.86, 122.54 and 119.78 (sp^2 carbons); 69.43 and 55.88 (sp^3 carbons). MS (ESI^+ in CH_3CN): 445 ($M+Na^+$).

RESULTS AND DISCUSSION

In this work, different zinc porphyrin-quinone dyads have been synthesized. In particular, **ZnTPP** and **ZnOEP** have been coupled with differently substituted anthraquinones to study the interaction between the D-A units upon excitation. Noteworthy, the quinone moiety was properly functionalized with imidazole, that can efficiently coordinate the zinc ion in the porphyrin macrocycle, thus allowing the formation of the dyad. Three different spacers were used to link the imidazole and the anthraquinone scaffold, in order to tune donor-acceptor distance and spacer flexibility. More in detail, a methylene unit was used to prepare the acceptor with the shortest distance, namely 2-imidazolylmethylanthraquinone (**AQ1**), obtained from the nucleophilic bimolecular substitution of 2-bromomethylanthraquinone with two equivalents of imidazole. An ester function was used to obtain (2-anthraquinonyl)methyl-6-imidazolylhexanoate (**AQ6**) from 2-hydroxymethylanthraquinone and 6-bromohexanoyl chloride. Bromine atom was then substituted with imidazole by a S_N2 reaction. A similar approach was used to synthesise (2-anthraquinonyl)methyl-*p*-imidazolylmethylbenzoate (**AQPh**), reacting 2-hydroxynaphthoquinone with *p*-bromomethylbenzoic acid, to form the ester function, with a reaction mediated by DCC and DMAP. Imidazole was then introduced by nucleophilic substitution of the bromine atom. All the dyads have been obtained in satisfactory yields and properly characterized.

Calculation of ΔG^0 for the photoinduced electron transfer. To check if the photoinduced electron transfer between the two electroactive units could occur in solution, the Gibbs energy for the mentioned process was calculated in dichloromethane. In particular, ΔG^0_{ET} value was estimated for all the dyads according to Rehm-Weller equation [24]:

$$\Delta G_{ET} = E\,(D^{+\cdot}/D) - E\,(A^{-\cdot}/A) - \Delta G_{00} - e^2/(4\pi\varepsilon_0\varepsilon R_C) \qquad \text{(eq. 1)}$$

To solve such equation, the zero-zero transition energies $\Delta G_{0,0}$ for **ZnTPP** and **ZnOEP** were estimated considering the emission wavelength in toluene (593 nm for **ZnTPP**, 573 nm for **ZnOEP**), while the redox potentials of the donor and acceptor moieties ($E^0(D^{+\cdot}/D)$ and $E^0(A/A^{-\cdot})$, respectively) were determined by cyclic voltammetry. The mean distance between the D-A units (R_C) was estimated from the optimized geometries, calculated using DFT models (see Supp. Info). R_C values for each acceptor were supposed to be the same for both porphyrins. The obtained data are listed in Table 1 and ΔG^0_{ET} values are collected in Table 2.

Table 1. Summary of the structural features for calculation of ΔG^0_{ET}

Donor	E^0 (V)	Acceptor	E^0 (V)	R_C (Å)
ZnTPP	0.75	**AQ1**	-0.92	9.6
ZnOEP	0.62	**AQ6**	-0.91	16.3
		AQPh	-0.92	11.9

Table 2. ΔG^0_{ET} values for the investigated porphyrin-anthraquinone complexes.

ZnTPP-AQ	ΔG^0_{ET} (eV)	ZnOEP-AQ	ΔG^0_{ET} (eV)
ZnTPP-AQ1	-0.59	**ZnOEP-AQ1**	-0.78
ZnTPP-AQ6	-0.53	**ZnOEP-AQ6**	-0.73
ZnTPP-AQPh	-0.55	**ZnOEP-AQPh**	-0.76

Obtained ΔG^0_{ET} values suggest that the photoinduced electron transfer can occur in all the synthesized dyads, being more favourable for the closest D-A units, as in the case of **AQ1** acceptor. As a matter of fact, for both porphyrins, the longer the distance between the units, the more disadvantaged the electron transfer. Conversely, a rigid acceptor (as **AQPh**) led to a more energetically favoured processes with respect to **AQ6** acceptor. Moreover, using the same acceptor unit, the photoinduced electron transfer process was favoured with **ZnOEP** donor with respect to **ZnTPP**, likely because of the electronic effect of the alkyl substituents on the porphyrin macrocycle.

***UV and Fluorescence Titration*.** The interaction between **ZnTPP** and **ZnOEP** with the imidazolyl functionalized anthraquinones was studied by UV-vis spectroscopy. Specifically, small amounts of a concentrated solution of the anthraquinone derivatives were added to a solution of each porphyrin, and the absorption spectra were registered (see Supp. Info). As an example, UV-vis titration of **ZnTPP** with **AQ1** is shown in Figure 1. It can be observed that in the presence of the acceptor unit, the intensity of the Soret band at 420 nm gradually decreased, while the band at 428 nm increased of intensity. Moreover, an intense red shift of the Q-bands was detected. The presence of two isosbestic points in each titration indicates the existence of only two species in solution, *i.e*. the free porphyrin and the dyad.

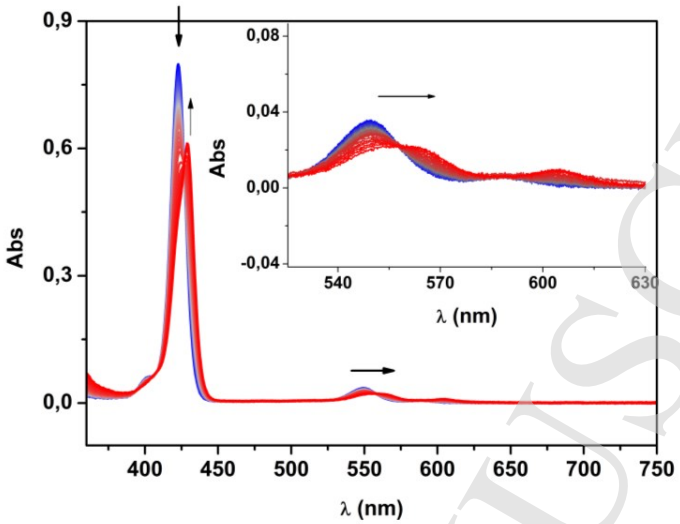

Fig. 1. UV-vis titration of **ZnTPP** (2.3 · 10^{-6} M) with **AQ1** (from 6.0 · 10^{-7} M to 4.0 · 10^{-5} M).

Using the Scatchard plot equation (eq. 2) [33], it was possible to calculate the binding constants for all the complexes, in order to estimate the concentration where the porphyrin is almost completely coordinated to the imidazole of the acceptor unit:

$$\frac{A_0 - A}{[AQ]} = -K_a \cdot (A_0 - A) + K_a \qquad \text{(eq. 2)}$$

In eq. 2, A indicates the absorbance of the porphyrin in the presence of the anthraquinone moiety, A_0 the absorbance in its absence, $[AQ]$ is the anthraquinone concentration and K_a is the association constant. Soret bands were chosen to analyze the absorption data, since anthraquinones do not absorb in that region.

As a comparison, in the case of **ZnTPP** and **ZnOEP**, which are fluorescent compounds, the binding constants was calculated also by fluorescence measurements. Therefore, the emission spectra were registered for the same solutions: the addition of increasing amounts of quinones to the porphyrin solutions resulted in fluorescence quenching (see Supp. Info). To prove that the quenching was not exclusively due to the complexation with imidazole, but it was also due to the occurring electron transfer between the D-A units, fluorescence titrations with 1-buthylimidazole were performed. The results show that in the absence of the quinone moiety, the quenching effect was significantly lower (see Supp. Info). Therefore, electron transfer between the porphyrins and anthraquinone units was effectively occurring.

Obtained data were fit by the Stern-Volmer equation (equation 3) [33]:

$$\frac{I_0}{I} = K_{SV} \cdot [AQ] + 1 \qquad \text{(eq. 3)}$$

where I is the fluorescence in the presence of the quencher (*i.e.* the anthraquinone derivative), I_0 the fluorescence in its absence, $[AQ]$ is the quencher concentration and K_{SV} represents the binding constant. Fluorescence titration of **ZnTPP** with **AQ1** and the corresponding Stern-Volmer plot are reported in Figure 2.

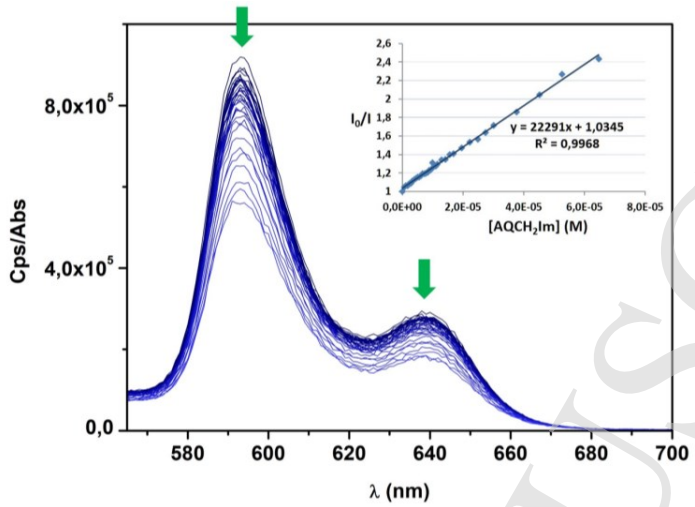

Fig. 2. Fluorescence titration of **ZnTPP** ($2.3 \cdot 10^{-6}$ M) with **AQ1** (from $6.0 \cdot 10^{-7}$ M to $4.0 \cdot 10^{-5}$ M) in toluene, normalised for the absorbance value. λ_{exc}= 550 nm. Inset: Stern-Volmer plot calculated at 593 nm.

Binding constants obtained from Uv-vis (K_a) and fluorescence (K_{SV}) measurements are summarised in Table 3.

Table 3. Binding constants for P-AQ complexes, obtained from Scatchard plot (K_a) and Stern-Volmer plot (K_{SV}), in toluene, at 25°C.

AQ	**ZnTPP**		**ZnOEP**	
	K_a (M^{-1})	K_{SV}	K_a (M^{-1})	K_{SV}
AQ1	2.6×10^4	2.2×10^4	6.6×10^3	7.6×10^3
AQ6	3.8×10^4	3.9×10^4	1.4×10^4	1.3×10^4
AQPh	2.4×10^4	2.2×10^4	1.2×10^4	1.1×10^4

From data reported in Table 3 it is possible to note that similar binding constant values were achieved with absorption and emission spectroscopies. Conversely to what expected from Gibbs free energy values reported in Table 2, for both porphyrins the highest binding constant was obtained with the **AQ6** acceptor. Moreover, with the same acceptor, higher constants have been achieved with **ZnTPP** donor species. To verify that the imidazole unit in the acceptor was the Zn-coordinating species, K_a for 1-buthylimidazole was measured. The obtained K_a was similar to those obtained with the imidazolyl-anthraquinone derivatives (9.7×10^3 M^{-1} for **ZnTPP**), thus confirming that the complexation occurred through the imidazole in the dyad.

As for ferrocene-naphthoquinone dyads [24], the fluorescence quenching indicates that an electron transfer from the donor moiety, *i.e.* the porphyrin, to the acceptor quinone, likely occurs. The linear correlation in the Stern-Volmer plot indicates that only one type of fluorophore is involved. However, the mechanism of the quenching can be either collisional or static [33]. To better understand the observed phenomena, femtosecond time resolved transient absorption spectroscopy has been performed, aiming at obtaining a clear evidence of the formation of radical cation or radical anion of the charge separated state P^{+}-AQ^{-}.

Transient absorption spectroscopy. Transient absorption spectra were recorded upon excitation of porphyrin, porphyrin-methylimidazole and **P-AQ** solutions. The complexes were obtained by addition of a toluene solution of the quinone (or 1-methylimidazole) to a solution of the porphyrin; the absorbance was checked before and after the laser excitation, to test the stability of the complexes. Concentrations of porphyrin and ligands were chosen in order to have an optical density value between 0.3 and 0.9 a.u. and to have less than 15% of free porphyrin, according to the measured K_a values.

The porphyrin Q bands correspond to $S_0 \rightarrow S_1$ transitions, whereas the Soret band to the $S_0 \rightarrow S_2$ ones. When porphyrins (and porphyrin complexes) were excited to the second excited state, the first process that occurred was the relaxation to the first excited state, S_1. Therefore, the observed decay was the one from the first excited state, even if the system was excited in correspondence of the Soret band. Hence, transient absorption spectra were recorded exciting both, at the Q band wavelength and at the Soret band, without noting any significant difference. Figure 3 shows the absorption spectra recorded at different times after the pump pulse at 430 nm, for **ZnTPP**, ZnTPP-1-methylimidazole (MeIm) and **ZnTPP-AQ1**.

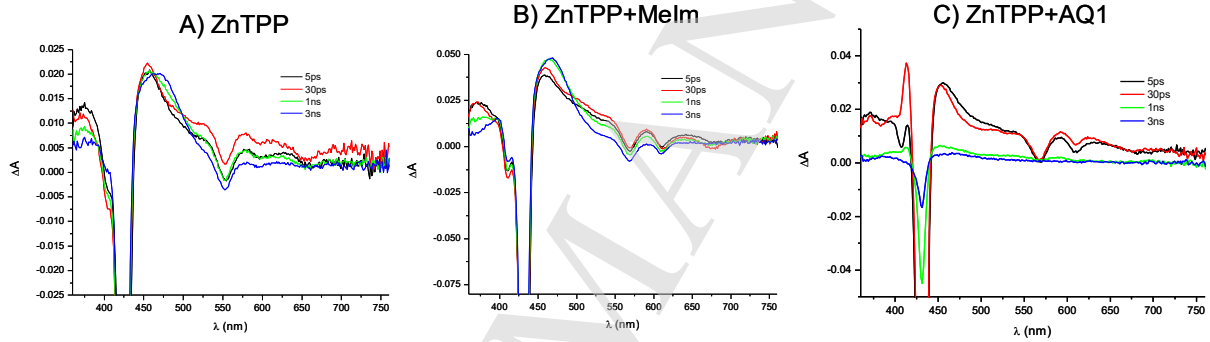

Fig. 3. Comparison between the transient absorption spectra in toluene of **ZnTPP** (A), ZnTPP-MeIm complex (B) and **ZnTPP-AQ1** complex (C) at different times, after excitation at 430 nm.

The transient absorption spectrum of **ZnTPP** shows a strong absorption band at 460 nm, due to the singlet excited state, ^{1*}**ZnTPP** [34]. With prolonged times (3 ns), such band was gradually red-shifted at 475 nm, because of the formation of the **ZnTPP** triplet excited state, ^{3*}**ZnTPP** [35]. Complexation of **ZnTPP** with imidazole does not significantly change the spectra: in fact, both, the singlet and the triplet excited states of the porphyrin were detected, whereas no other absorption bands were observed. In the case of **ZnTPP-AQ1** dyad, the formation of ^{3*}**ZnTPP** was less pronounced. Moreover, a sharp absorption band appeared around 410 nm (see Figure 3c, red line). This latter can be attributed to the formation of the porphyrin radical cation, **ZnTPP**$^{+\cdot}$. As a matter of fact, a similar band (cantered at 407 nm) was observed in spectroelectrochemical measurements of the porphyrin in dichloromethane (see Supp. Info). As a confirmation, transient absorption spectra of **ZnTPP** in the presence of 9,10-anthraquinone as acceptor have been recorded, since such molecule cannot interact with the zinc porphyrin. As a result, similar spectra to those obtained for the **ZnTPP** alone have been recorded, proving that no electron transfer occurred by an intermolecular process. Moreover, data suggested that, in the presence of the anthraquinone moiety, after the excitation at 420 nm, the formation of the singlet excited state evolved into a charge separated state, **ZnTPP**$^{+}$**AQ**$^{-}$, that competes with the intersystem crossing (Scheme 1). The lifetime of the charge separated state, calculated by a triexponential decay fit of the kinetic trace at 410 nm (Figure 4), was 350 ps for **ZnTPP-AQ1**, whereas it increased up to 1.1 ns for **ZnTPP-AQ6** (Table 4). Therefore, the long distance between the porphyrin and

the anthraquinone core stabilised the charge separated state in **ZnTPP-AQ6**, likely reducing the charge recombination process. The best fitting for **ZnTPP-AQPh** data at 410 nm was biexponential and no similar decays could be detected. A reasonable explanation could be that in the presence of a rigid spacer, the approach of the quinone to the porphyrin is hampered. Notably, the transient spectrum of the **ZnTPP-AQ1** dyad, where the quinone is quite close to the porphyrin, is characterized by the most intense signal at 410 nm. In other words, the proximity of the donor and acceptor moieties could promote the electron transfer process, whereas a longer distance between them could prevent the charge recombination, thus extending the charge separated state lifetime.

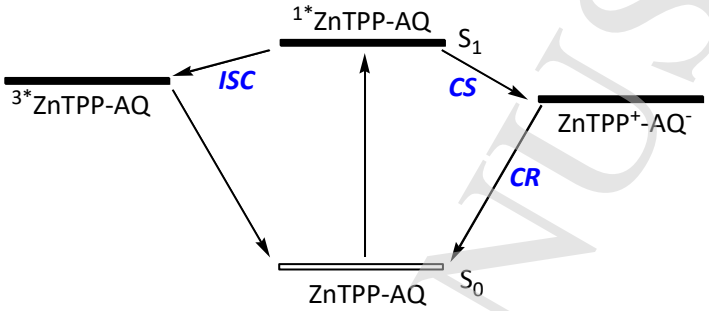

Scheme 1. Proposed ET transfer processes for **ZnTPP-AQ** systems.

Table 4. Kinetic parameters obtained for the investigated **ZnTPP-AQ** complexes, at 410 nm, at 25°C.

Compound	A_1 (%)	τ_1 (ps)	A_2 (%)	τ_2 (ps)	A_3 (%)	τ_3 (ps)	χ^2
ZnTPP-AQ1	-33	83	-18.4	7	48	356	0.002
ZnTPP-AQ6	-53	210	-13	27	34	1130	0.001
ZnTPP-AQPh	-85	229	-15	26	-	-	0.0015

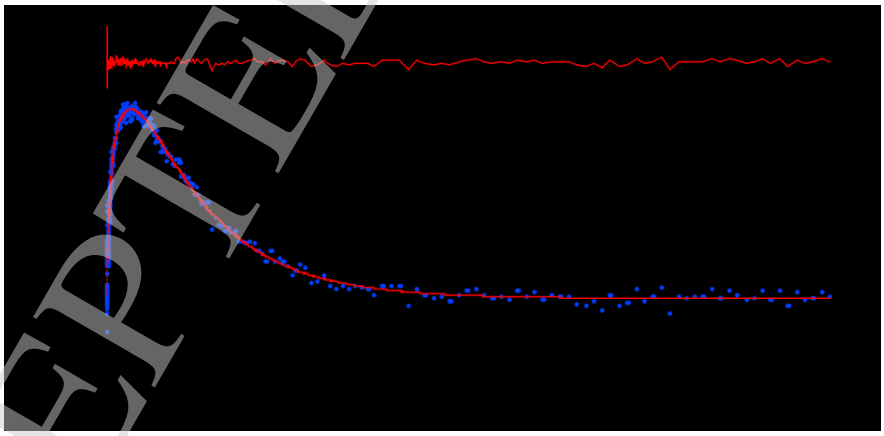

Fig. 4. Kinetic trace (blue dots) and fitting (red line) at 410 nm for **ZnTPP-AQ1** complex. Excitation wavelength: 430 nm.

A further confirmation of the occurring electron transfer can be achieved by studying the kinetic decay at 550 nm, corresponding to the signal of $AQ^{\bullet-}$ in accordance with spectroelectrochemistry measurements of **AQ1** in dichloromethane

(see Supp. Info). Although the signal of the singlet excited state of the porphyrin hides the signal of the $AQ^{\bullet-}$, it is possible to observe that such decay remains unchanged when the zinc-porphyrin is coordinated with methylimidazole, whereas it is faster in the presence of **AQ1**. Kinetic decays at λ=550 nm are reported in Figure 5 and the corresponding fitting data are collected in Table 5.

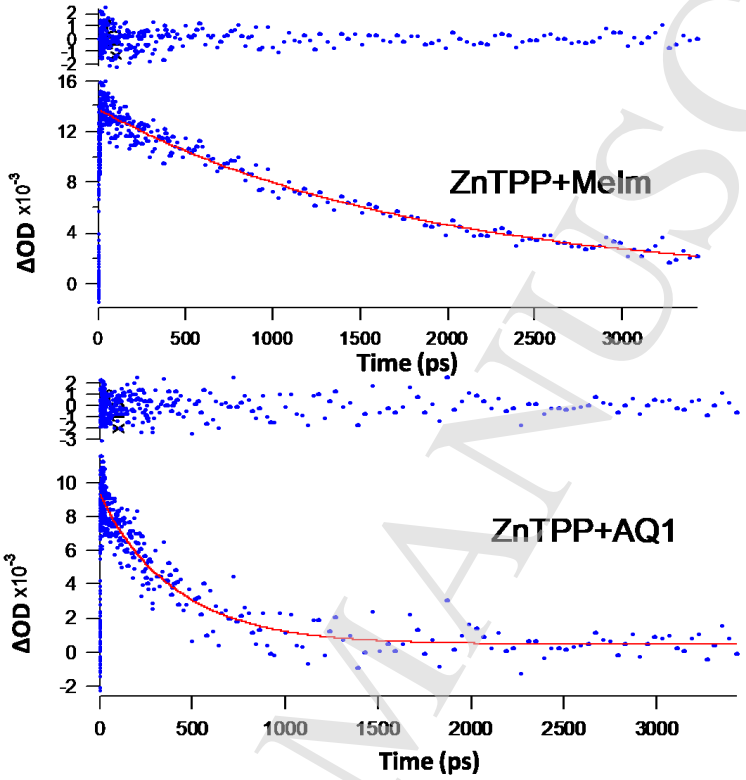

Fig. 5. Kinetic decay for ZnTPP-MeIm and **ZnTPP-AQ1** at 550 nm. λ_{exc}=430 nm.

Table 5. Kinetic parameters obtained at λ=550 nm for some of the ZnTPP-AQ complexes, at 25°C.

Compound	A_1 (%)	τ_1 (ps)	A_2 (%)	τ_2 (ps)	χ^2
ZnTPP	100	1272	-	-	0.0001
ZnTPP-MeIm	100	1796	-	-	0.0002
ZnTPP-AQ1	98	410	2	39	0.0003

Femtosecond transient absorption spectra for **ZnOEP-AQ** dyads were registered exciting in the Q band region, at 530 nm (see Supp. Info). In the case of **ZnOEP** dyads, no other absorption bands were observed with respect to the porphyrin alone. However, it is possible to observe changes in the kinetic decays of the spectra at 380 nm, as shown in Figure 6, where the kinetic curves of the different dyads are compared. At that wavelength, the radical cation of the porphyrin should absorb, as already observed by spectroelectrochemical measurements.

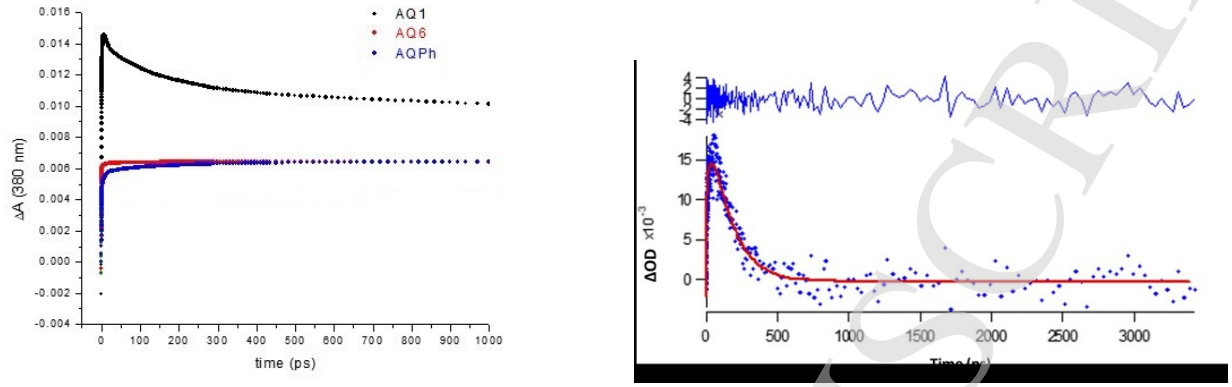

Fig. 6. Kinetic decays for **ZnOEP** complexes at λ=380 nm (left) and fitting of the absorption data at λ=380 nm for **ZnOEP-AQ1** (right).

As in the case of **ZnTPP**, the evidence of weak bands might be due to the formation of the charge separated state, **ZnOEP^{+}AQ^{-}**. The kinetic decays at 380 nm were triexponentially fitted in order to have an idea of the lifetime of all the investigated dyads (Table 6). The lifetime of the radical cation was 140 ps for the short quinone **AQ1** and, similarly to **ZnTPP** complexes, it increased with increasing distances between the donor and the acceptor. Conversely, the rigid spacer in **AQPh** determined a shorter, but still remarkable, lifetime of 1.3 ns. The lower reduction potential of **ZnOEP** with respect to **ZnTPP**, due to the presence of the electron donating group in the aromatic core, together with the lower steric hinderance of ethyl substituents, could make the difference in terms of energetically favoured electron transfer. In fact, also the way porphyrins approach the acceptor unit can be influenced by the different steric hinderance of substituents.

Table 6. Kinetic parameters obtained for the fitting of **ZnOEP-AQ** complexes at 380 nm.

Sample	A_1 (%)	τ_1 (ps)	A_2 (%)	τ_2 (ps)	A_3 (%)	τ_3 (ps)
ZnOEP+AQ1	47	140	-29	37	-23	2
ZnOEP+AQ6	43	911	-14	156	-42	2.5
ZnOEP+AQPh	50	1285	-28	199	-21	3

CONCLUSION

In this work, new **P-AQ** dyads have been prepared. In particular, **ZnTPP** and **ZnOEP** were used as electron donor units, coupled with different imidazolyl functionalised anthraquinones as acceptors. Analysis of Gibbs free energy demonstrated that the photoinduced electron transfer was energetically favoured for all the synthesised dyads. UV-vis and fluorescence studies allowed to directly follow the association between the D-A units and to measure the binding constants. Association (Ka) and Stern-Volmer (K_{SV}) constants were in the range $6.6 \cdot 10^3$ - $3.9 \cdot 10^4$ M^{-1} for all the dyads.

Femtosecond absorption spectroscopy of the dyads was performed. In the case of **ZnTPP**, the formation of the charge separated (CS) state was indicated by the formation of a new absorption band due to the radical cation of the porphyrin. This band was particularly evident for **ZnTPP-AQ1** complex and the measured decay lifetime was about 300 ps. For longer D-A distances, as in **ZnTPP-AQ6** dyad, a similar but slower decay was detected at 410 nm with a longer lifetime.

Considering the **ZnOEP** complexes, the kinetic decays and the detection of a new absorption band (corresponding to the radical cation) also suggested the formation of the CS state. Obtained results indicated a strong correlation between the spacer length and flexibility with the CS state lifetime.

Furthermore, the observed differences for the dyad composed by **ZnTPP** or **ZnOEP** donor with **AQPh** acceptor have been attributed both, to electronic and steric effect of substituents. In fact, in the case of **ZnOEP**, alkyl groups lower the oxidation potential of the porphyrin, and they can also influence the way porphyrin approaches the acceptor unit.

To conclude, in this work we found that, although at the ground state **ZnOEP** exhibited a lower oxidation potential than **ZnTPP**, at the excited state the latter resulted the most efficient electron donor unit in the studied P-AQ dyads. Therefore, modulation of porphyrin substituents, as well as D-A spacer nature (length, flexibility), allows to tune the electron transfer properties of the dyads.

REFERENCES

1. Hou Y, Zhang X, Chen, K, Liu D, Wang, Z, Liu Q, Zhao J, Barbon A. *J. Mater. Chem. C* 2019; **7**: 12048-12074.
2. Cupellini L, Giannini S, Mennucci B. *PhysChemChemPhys* 2018; **20**: 395-403.
3. Wu Z-Y, Yang S-Y. *J. Mol. Struct.* 2019; **1188**: 244-254.
4. Stasyuk AJ, Stasyuk OA, Sola M, Voityuk AA. *Chem. Eur. J.* 2019; **25**: 2577-2585.
5. Nikolaou V, Plass F, Planchat A, Charisiadis A, Charalambidis G, Angaridis PA, Kahnt A. Odobel F, Coutsolelos AG. *Phys. Chem. Chem. Phys.* 2018; **20**: 24477-24489.
6. Lu X-J, Zhang C-R, Shen Y-L, Wu Y-Z, Liu Z-J, Chen H-S. *J. Mol. Struct.* 2018; **1173**: 398-405.
7. Ovchenkova EN, Bichan NG, Lomova TN. *Russ. J. Inorg. Chem.* 2018; **63**: 391-399.
8. Solis C. Ballatore, MB, Suarez MB, Milanesio ME, Durantini EN, Santo M, Dittrich T, Otero L, Gervaldo M. *Electrochim. Acta* 2017; **238**: 81-90.
9. Gupta N, Naqvi S, Jewariya M, Chand S, Kumar R. *J. Phys. Org. Chem.* 2017; **30**: e3685.
10. Lim GN, Obondi CO, D'Souza F. *Angew. Chem. Intern. Ed.* 2016; **55**: 11517-11521.
11. Ovchenkova EN, Bichan NG, Lomova TN. *Russ. J. Org. Chem.* 2016; **52**: 1503-1508.
12 Kelson MMA, Bhosale RS, Ohkubo K, Jones LA, Bhosale SV, Gupta A, Fukuzumi S, Bhosale SV. *Dyes Pigments* 2015; **120**: 340-346.
13. Natali M, Ravaglia M, Scandola F, Boixel J, Pellegrin Y, Blart E, Odobel F. *J. Phys. Chem. C* 2013; **117**: 19334-19345.
14. Cheng F, Wang H-H, Kandhadi J, Zhao F, Zhang L, Ali A, Wang H, Liu H-Y. *J. Phys. Chem. B* 2018; **122**: 7797-7810.
15. Balsukuri N, Gupta I. *Dyes Pigments* 2017; **144**: 223-233.
16. Das S, Bhat HR, Balsukuri N, Jha PC, Hisamune Y, Ishida M, Furuta H, Mori S, Gupta I. *Inorg. Chem. Front.* 2017; **4**: 618-638.
17. Balsukuri N, Das S, Gupta I. *New J. Chem.* 2015; **39**: 482-491.
18. Temelli B, Gunduz M, Yuksel D. *Tetrahedron* 2018; **74**: 4476-4488.
19. Tao M-L, Liu D-Z, Zhang M-H, Zhou X-Q, Li L-H. *J. Porphyrins Phthalocyanines* 2010; **14**: 219-226.
20. Wijesinghe CA, Niemi M, Tkachenko NV, Subbaiyan NK, Zandler ME, Lemmetyinen H, D'Souza F. *J. Porphyrins Phthalocyanines* 2011; **15**: 391-400.

21. Perchanova M, Kurreck H, Berg A. *J. Phys. Chem. A* 2015; **119**: 8117-8124.
22. Melomedov J, Ochsmann JR, Meister M, Laquai F, Heinze K. *Eur. J. Inorg. Chem.* 2014; 1984-2001.
23. Duvva N, Ramya AR, Reddy G, Giribabu L. *J. Porphyrins Phthalocyanines* 2019; **23**: 628-638.
24. Sabuzi F, Coletti A, Pomarico G, Floris B, Galloni P, Conte V. *J. Organomet. Chem*. 2019; **885**: 49-58.
25. Sabuzi F, Lentini S, Sforza F, Pezzola S, Fratelli S, Bortolini O, Floris B, Conte V, Galloni P. *J. Org. Chem.* 2017; **82**: 10129-10138.
26. Bonomo M, Sabuzi F, Di Carlo A, Conte V, Dini D, Galloni P. *New J. Chem.* 2017; **41**: 2769-2779.
27. Sabuzi F, Armuzza V, Conte V, Floris B, Venanzi M, Galloni P, Gatto E. *J. Mater. Chem. C* 2016; **4**: 622-629.
28. Coletti A, Lentini S, Conte V, Floris B, Bortolini O, Sforza F, Grepioni F, Galloni P. *J. Org. Chem.* 2012; **77**: 6873-6879.
29. Satake A, Kobuke Y, *Tetrahedron,* 2005; **61**: 13-41.
30. Satake A, Shoji O, Kobuke Y, *J. Organomet. Chem*. 2007; **692**, 635–644.
31. Pasternack RF, Francesconi L, Raff D, Spiro E. *Inorg. Chem*. 1973; **12**: 2606-2611.
32. Jones FN, Lu DD-L, Pechacek J, Kangas SL *Ind. Eng. Chem. Prod. Res. Dev.* 1986; **25**: 385-389.
33. Lakowicz JR. *Principles of fluorescence spectroscopy*, (3rd edn), Springer, 2006.
34. Kadish KM, Shiue LR, Rhodes RK, Bottomley LA. *Inorg. Chem*. 1981; **20**: 1274-1277.
35. Hayes RT, Walsh CJ, Wasielewski MR. *J. Phys. Chem. A* 2004; **108**: 2375-2381.